12[th] International Conference on Applications of Statistics and Probability in Civil Engineering, ICASP12
Vancouver, Canada, July 12-15, 2015

Response of Buried Pipes Taking into Account Seismic and Soil Spatial Variabilities

Sidi Mohammed Elachachi
Associate-Professor, GCE Department, I2M, Univ. of Bordeaux, Bordeaux, France.

Humberto Yanez-Godoy
Associate-Professor, GCE Department, I2M, Univ. of Bordeaux, Bordeaux, France.

ABSTRACT: Heavy damage to pipelines has occurred in many strong earthquakes. Because pipes extend over long distances parallel to the ground, their supports undergo differential motions during an earthquake. Furthermore the soil spatial variability and the soil-pipe interaction contribute to the appearance of additional stresses and deformations. Herein, a frequency domain spectral analysis for obtaining the response of pipes to correlated or partially correlated non stationary random ground motion and spatially random soil is presented. The space-time variability of the ground motions and of the soil spatial variability are modeled following a stochastic description through random process (fields) and spectral analysis. The key results are that soil heterogeneity induces significant effects (differential settlements, bending moments, counter-slopes) that cannot be predicted if soil homogeneity is assumed. The spatial variation of the ground motion could increase locally the structural response depending on the soil-structure interaction and the pipe-joint stiffness ratio in segmented pipes.

1. INTRODUCTION

Dysfunctions and failures of buried pipe networks like water supply or sewer networks under seismic actions are principally due to three main factors: the spatial variation of seismic ground motions, the heterogeneity of geotechnical conditions and the soil-pipe interaction.

Because pipes extend over long distances parallel to the ground, their supports undergo different motions during an earthquake. This spatial variation of seismic ground motions lead to differential motion which could increase and modify the seismic behavior of pipes beyond the response expected if the input motions at the pipesô supports were assumed to be identical. Harichandran (1990) had shown that the assumption of fully coherent support motions may be over-conservative for some bridges which are structures whose longitudinal dimension is predominant and under-conservative for others. Soliman and Datta (1994) showed that the inclusion of the spatial correlation of the ground motion in the seismic analysis of bridges lead to changes in the response by varying degrees depending upon the type of the power spectral density function of the ground motion used.

The second cited factor is the heterogeneity of geotechnical conditions and soil properties in the longitudinal direction which can be considered as spatially structured and a result of its natural or man-made fabric (deposit processes, compaction processes...). Last factor, the interactions between the pipe and the geologic media underlying and surrounding it have to be taken into account when the soil or the foundation medium is not very firm.

The space-time variability of the ground motions and of the soil spatial variability are modeled following a stochastic description through random process (fields) and spectral analysis:

- the random field of seismic ground motions is described by means of both the cross spectral density at two stations *j* and *k* on the ground surface and a specified point estimate power spectral density (Zerva 2009) which must be response spectrum compatible (see §3). It results in two distinct effects (Der Kiureghian 1996): (1) a loss of coherence of the seismic movement due to multiple refractions and reflexions of the seismic waves along their paths, named incoherence effect, (2) a difference in arrival times of the seismic waves at the various recording stations due to the variation of their apparent propagation velocity, named wave passage effect.

- Another effect, namely the site effect is taken into account in this paper considering that the soil spatial variability is modelled as a random field of soil properties by means of the theory of local average developed by VanMarcke (Van Marcke 1983); it is defined by three properties: the mean value of the soil property or the soil-pipe interaction property, its variance and its scale (or length) of correlation which describes the spatial structure of correlation (i.e. the distance above which the local properties at two points can be assumed to be independent).

2. EQUATION OF MOTION

In this analysis the pipe-soil interaction is modelled by an elastic foundation with uniformly distributed springs and dashpots as shown in Figure 1. The spring stiffness and damping coefficients of the dashpots are derived by combining Mindlinõs static analysis of the soil pressure at a depth within the soil and the soil impedance functions. The stiffness and damping coefficients of the matrices corresponding to the degrees of freedom (d.o.f) are coupled unlike the condition of Winklerõs bed. In this buried pipe model, the beam segments of equal length are aligned and connected by identical joints.

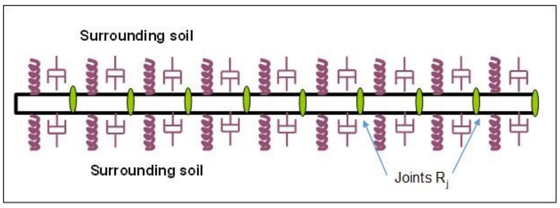

Figure 1: Soil-segmented pipes model

The equation of motion of segmented pipes with joints is, Eq. (1):

$$M_t \ddot{X}^t(t) + C_t \dot{X}^t(t) + K_t X^t(t) = P(t) \qquad (1)$$

With:

$$\begin{cases} M_t = M_p \\ C_t = C_p + C_s \\ K_t = K_p + K_s + K_j \\ P(t) = C_s \dot{X}_g(t) + K_s X_g(t) \end{cases} \qquad (2)$$

Where:

K_p, K_s and K_j are respectively the stiffness matrices of the non-support degrees of freedom (d.o.f), of the support d.o.f and of the joints, C_p and C_s are the damping matrices, M_p the mass matrix of the pipe, X_t the vector of total displacements of non-support d.o.f, X_g the vector of input ground displacement. The dots indicate differentiation with respect to time.

As mentioned by Datta (Datta, 2010), the inertia forces are mainly resisted by the surrounding soil in the case of buried structures, the total displacement of the structure becomes important for finding the stresses in the structure. Because of this assumption, the buried pipes are under deformation control as the stresses induced in the structures are primarily governed by the deformation of the soil due to the earthquake. The ground motion is considered as being incoherent. The buried structures are heavily damped because of the embedment within the soil. As a result, the frequency amplification is insignificant (unlike over ground structures).

The response of the soil-pipes system is performed here according to a frequency domain spectral analysis. One of the advantages of this method is that the size of the problem and the computing time can be drastically reduced without compromising much on the accuracy of the results. The frequency domain spectral analysis treats the ground motion as a stationary (or weakly stationary) random process. It uses Fast Fourier Transform (FFT) which provides a good understanding of the characteristics of the ground motion. Using the principles of random vibration analysis, it provides the power spectral density function (PSD) of any response quantity of interest for a given PSD of ground motion as the input. The root mean square response and expected peak response are obtained from the moments of the PSD of response (Datta, 2010).

3. SEISMIC GROUND MOTION WITH SPATIAL VARIATION

Seismic codes define the seismic action by means of the evaluation of the maximal response of a single-degree-of freedom (SDOF) system through a Response Spectrum (RS). The RS depends on the seismicity of the site, on the soil condition, on the importance of the structure and also on the assumed ductility of the lateral load resisting system and on the limit state under consideration (Navarra *et al.*, 2013).

To respect a prescribed RS, one need to generate different ground motion representation by means of response-spectrum compatible artificial accelerograms. They are samples of a zero-mean Gaussian non stationary process, fully characterized by their PSD function. Insofar the seismic codes do not define this PSD function, a first task was to build ground acceleration, ground velocity and ground displacement PSD functions.

3.1. PSD consistent functions with EC8 Response Spectra

In this paper, we used the analytical PSD model proposed by Navarra (Navarra *et al.*, 2013), coherent with any form of RS and especially Eurocode 8. The model is based on few parameters, related to the parameters that define the RS itself.

$$RS(T)=\begin{cases} a_g S\left[1+\dfrac{T}{T_B}(2{,}5\eta-1)\right] & 0\le \mathrm{T}\le \mathrm{T_B} \\ 2{,}5 a_g S\eta & \mathrm{T_B}\le \mathrm{T}\le \mathrm{T_C} \\ 2{,}5 a_g S\eta\dfrac{T_C}{T} & \mathrm{T_C}\le \mathrm{T}\le \mathrm{T_D} \\ 2{,}5 a_g S\eta\dfrac{T_C T_D}{T^2} & \mathrm{T_D}\le \mathrm{T}\le 4s \end{cases} \quad (3)$$

T is the SDOF period, a_g the ground acceleration, η coefficient equals to 1 if the damping coefficient is equal to 5% and *S* is related to soil type. For a soil type *A* (Figure 2), *S*, T_B, T_C, and T_D, are equal respectively to 1, 0.05 s, 0.25 s and 1.2 s (according to EC8). ω_B, ω_C, and ω_D are their dual natural frequencies. These values lead, taking everything into account, to values of G_1 and G_2 equal respectively to 3.10^{-3} m²/(s.rad) and $9.3.10^{-3}$ m²/(s.rad). The other parameters are in turn: $e_1 = 10/3$, $e_2 = 2/3$, $e_3 = -4/3$, $e_4 = -8/3$.

$$S(\omega)=\begin{cases} G_1\left[\dfrac{\omega}{\omega_D}\right]^{e1} & 0\le\omega\le\overline{\omega}_D \\ G_2\left[\dfrac{\omega}{\omega_C}\right]^{e2} & \overline{\omega}_D\le\omega\le\omega_C \\ G_2\left[\dfrac{\omega}{\omega_C}\right]^{e3} & \omega_C\le\omega\le\omega_D \\ G_2\left[\dfrac{\omega_B}{\omega_C}\right]^{e3}\left[\dfrac{\omega}{\omega_B}\right]^{e4} & \omega\le\omega_B \end{cases} \quad (4)$$

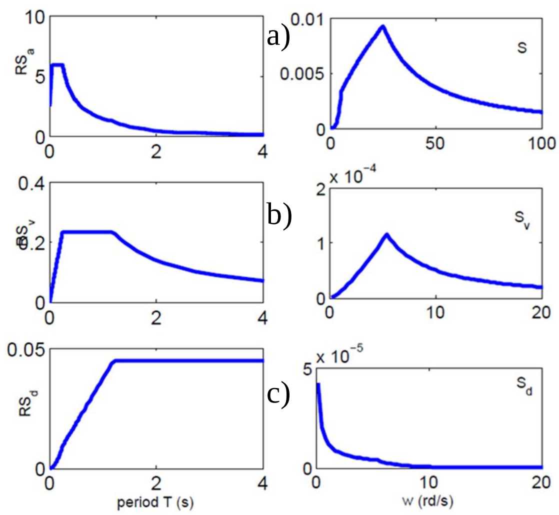

Figure 2: Response spectrum (left) and power spectral density (right) for: a) acceleration, b) velocity and c) displacement.

And:

$$\overline{\omega}_D=\left(\frac{G_2\omega_D^{e1}}{G_1\omega_C^{e2}}\right)^{\left(\frac{1}{e1-e2}\right)} \quad (5)$$

$$S_d(\omega) = \frac{S}{\omega^4}; \quad S_v(\omega) = \frac{S}{\omega^2} \tag{6}$$

The estimated PSD functions S, S_v and S_d are sharply peaked and are very different from those proposed by Der kiureghian and Neuenhofer (1992) or Hindy and Novak (1980) for natural earthquakes. The generated earthquakes which are firstly stationary are converted to non-stationary ones through their multiplication with an amplitude modulating (envelope) function.

3.2. Coherency function

The spatial variation of the seismic movement is characterized by the cross power spectral density function of soil accelerations. This function is related to the power spectral density function by the coherency function γ. Among the variety of parametric coherency functional forms (Zerva, 2009), we use in this paper the one proposed by Harichandran and Vanmarcke (1986):

$$|\gamma(\zeta,\omega)| = A\exp\left\{-\frac{2\zeta(1-A)}{ak}\sqrt{1+\left(\frac{\omega}{\omega_0}\right)^b}\right\} + (1-A) \tag{7}$$

The cross spectral density function between two points i and j is thus obtained by Eq. (8):

$$S_{ij}(\omega) = \gamma(\zeta,\omega)\sqrt{S_i(\omega)S_j(\omega)} \tag{8}$$

The parameters A, ζ, a, k, b and ω_0 are those proposed by Harichandran and Vanmarcke (1986). The statistical properties of the cross spectral density are similar to those of the power spectrum.

4. SOIL SPATIAL VARIABILITY

Since the role of the longitudinal soil variability appears essential, we chose to model it by using the theory of the local average of a random field developed by VanMarcke (1983). The random field of the impedance coefficients (soil stiffness and damping) are defined by three properties each one: mean value m, variance σ^2 and scale (or length) of correlation l_c. The selected PSD function of the soil impedance is that of an exponential random field (Eq. 9). The correlation length depends on the soil characteristics (modulus, porosity, water content...) and on the direction (horizontal or vertical).

$$S_{soil}(\omega) = \frac{\sigma^2 l_c}{\pi(4 + l_c^2\omega^2)} \tag{9}$$

It is assumed here that the impedance coefficients have similar correlation lengths. Another hypothesis that could be considered strong is the fact that even though we knows that the impedance coefficients are frequency dependent, they will be considered in this paper as independent of frequency (true enough for high pipe length diameter ratio).

Figure 3 shows the power spectral density function for three different correlation lengths.

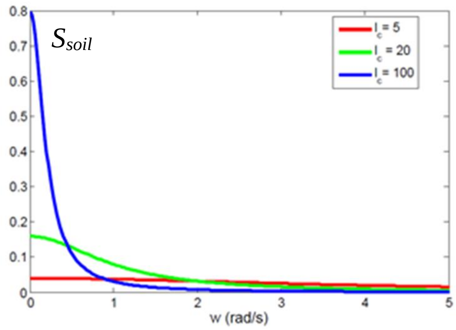

Figure 3: Power spectral density of soil impedance coefficients for three values of correlation length l_c

5. FOLLOWED APPROACH

5.1. Maximal responses

The solution of Eq. (1) using frequency domain spectral analysis can be expressed as:

$$X^t(\omega) = H(\omega)P(\omega) \tag{10}$$

P(ω) is the vector of stationary random process (see Eq (2)). For a multipoint supports, after some straightforward derivations, the PSD $S_X{}^t$ that we obtained and which is a non-classical equation is:

$$S_{X^t}(\omega) = HS_{PP}H^{*T} \tag{11}$$

$$S_{X^t}(\omega) = [H_1; H_2]\begin{bmatrix} S_{p11} & S_{p12} \\ S_{p21} & S_{p22} \end{bmatrix}\begin{bmatrix} H_1^{*T} \\ H_2^{*T} \end{bmatrix} \tag{12}$$

$$\begin{cases} S_{p11} = C_S C_s^T S_{\dot{X}g} \ ; \ S_{p12} = C_S K_s^T S_{\dot{X}gXg} \\ S_{p21} = K_S C_s^T S_{Xg\dot{X}g} ; \ S_{p22} = K_S K_s^T S_{Xg} \end{cases} \tag{13}$$

In which:

$H_1(\omega)$ *and* $H_2(\omega)$ are complex frequency response function matrices corresponding respectively to velocity and displacement, $H(\omega)^*$ indicates the complex conjugate of $H(\omega)$. $S_{\dot{X}gXg}$ and $S_{Xg\dot{X}g}$ are the cross PSD matrix between velocity and displacement ground motions.

$$H_1(\omega_j) = (i\omega_j K_t - \omega_j^2 C_t)(K_t - M\omega_j^2 + i\omega_j C_t)^{-1}$$

And (14)

$$H_2(\omega_j) = (K_t + i\omega_j C_t)(K_t - M\omega_j^2 + i\omega_j C_t)^{-1}$$

ω_j is the jth frequency component of the excitation vector *P*.

Using the normal mode theory, the equation of motion, Eq. (1) is decoupled into a set of *n* uncoupled equations of motion and therefore Eq. (12) becomes more simplified and could be decomposed as:

$$\begin{aligned} S_{X^t}(\omega) = A^T S_{Xg} A + \varphi_\beta^T S_{X^t}\varphi_\beta + \\ A^T S_{XgX^t}\varphi_\beta + \varphi_\beta^T S_{X^tXg} A \end{aligned} \tag{15}$$

A is a coefficient vector denoting the response quantity of interest for unit displacements applied at the supports, ϕ_β particular modal vectors. Performing integration of Eq. (15) over the entire range of frequencies, writing the mean peak value of response *R* (non-support displacement, bending moment,...) as peak factor multiplied by the standard derivation of the response and assuming all peak factors to be the same, the following expression for the mean peak response of *R* may be obtained (Datta, 2010; Der Kiureghian and Neuenhofer 1992):

$$E[\max(R(t))] = \begin{bmatrix} D^T l_{\dot{X}g} D + D^T l_{\dot{X}gXg}\varphi_\beta + \\ + \varphi_\beta{}^T l_{Xg}\varphi_\beta + \varphi_\beta{}^T l_{Xg\dot{X}g} D \end{bmatrix}^{1/2} \tag{16}$$

D^T is related to the peak ground displacement at the *ith* support, φ_β is related to the ordinate of the displacement response spectrum for the ground motion at support *i* corresponding to time period T_j, $l_{\dot{X}g}$ is the correlation matrix between the velocities at the supports, $l_{\dot{X}gXg}$ is the correlation matrix between the velocities and the displacements at the supports, $l_{Xg\dot{X}g}$ is the transpose of $l_{\dot{X}gXg}$, and l_{Xg} is the correlation matrix between all displacements at the supports.

This approach enables in theory to achieve results with a reduced calculation time insofar as one does not need to resolve the equation of motion in the time domain (Elachachi *et al.* 2010).

5.2. Soil variability and Monte Carlo simulations

In Eq. (10) to Eq. (16) the soil is considered as homogeneous or at best with piecewise constant properties. In order to take into account its spatial variability, through the variability of its impedance coefficients, Monte Carlo simulations (MCS) are used to incorporate this aspect. MCS is suitable for probabilistic analyses, but a large number of samples is required. We use here an improved MCS method namely Latin hypercube sampling method (MacKay *et al.* 1979). Therefore MCS allows to build probability distribution functions of the maximum responses (displacements, bending moments, counter-slopes or joints opening).

6. CASE STUDY

6.1. Characteristics of the pipe's section

We consider a reinforced concrete material for the pipe (Young modulus E_p = 25 GPa) with an exterior diameter D_{ext}= 1 m, a thickness of 0.08 m, made of a set of 50 pipes with unit length (L_p=6m) and buried depth of 2.5 m. It rests on a soil whose impedance coefficients are: Winkler (spring) coefficient with a mean of 10 kN/m^3 and damping coefficient of 5 kN.m^{-1}.s and both with a coefficient of variation of 25%. This type of configuration corresponds to a pipe-soil ratio of 0.678. It must be noted that the pipe geometry intervenes as well in the expression of inertia I_p as in that of the Winkler coefficient. The pipes are subjected to a deterministic uniform loading of 150 kN/m and to seismic load compatible with the Eurocode 8. Extensive parametric studies of the pipe response were conducted and are presented here for three issues: soil heterogeneity, coherency function and joint-pipe effects.

6.2. Effect of Soil heterogeneity

The PSD is supposed to be the same in all supports as soils conditions are identical. To analyze the effects of soil heterogeneity, five different bedding conditions are considered:

- Case 1a: the same soil type B of EC8 (very dense sand with a shear wave velocity V_s in the top 30 m of 600 m/s) is beneath the all the pipe with a correlation length equal to 10 m,
- Case 1b: the same soil type B with a correlation length equal to 100 m,
- Case 2a: two types of soils separated by vertical boundary and therefore two response spectrums: type B along 150 m and type D (soft cohesive with a shear wave velocity V_s of 200 m/s) along the remaining 150 m. The correlation lengths are respectively equal to 10 m for the two zones,
- Case 2b: same as Case 2a with correlation lengths of 100 m for the two zones,
- Case 2c: same as Case 2a with correlation length of 10 m for the soft soil and 100 m for the stiff soil.

Figure 4 shows the transfer functions H between the ground motion velocity (to which the equivalent seismic forces applied at the supports of the pipe are proportional) and the total displacement in the middle of the pipe for Case 1a. Typical plots for the PSD of respectively displacement and bending moment in the middle point of the pipe are shown in Figures 5 and 6.

The effect of the number of modes on the response quantities of interest was analyzed.

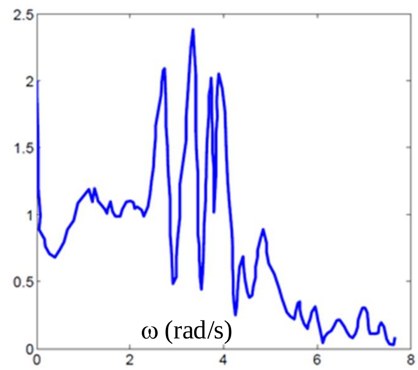

Figure 4: Transfer function H in the middle of the beam for Case 1a.

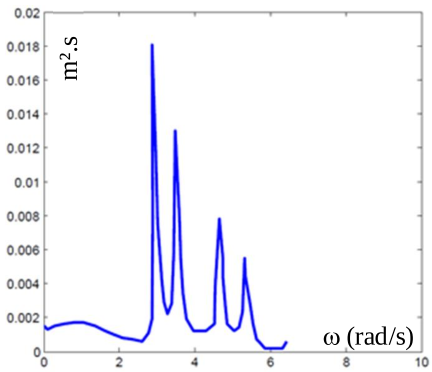

Figure 5: PSD of the displacement in the middle point of the pipe for Case 1a.

It is seen that the first seven modes practically govern the overall response for displacement, whereas practically ten modes are required to compute the bending moments correctly for all the cases. The responses are thus obtained by considering the first ten symmetric and antisymmetric modes separately, and then by considering them together. The results show that the contributions of the symmetric modes are higher than those of the antisymmetric modes to the overall response. A number of 10^5 Monte Carlo simulations have been conducted. Table 1 shows the (mean) maximal responses for the five cases.

Figure 7 depicts the cumulative density functions of the maximal bending moment and the maximal displacement for the five cases. The mean and standard deviation (between brackets) values are shown on Table 1.

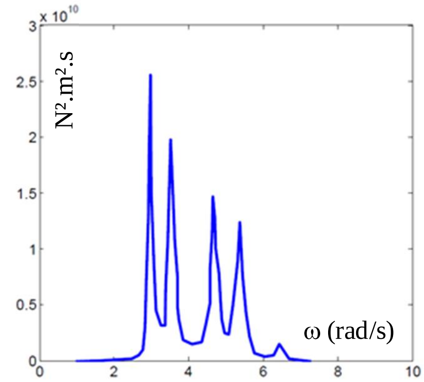

Figure 6: PSD of the bending moment in the middle point of the pipe for Case 1a.

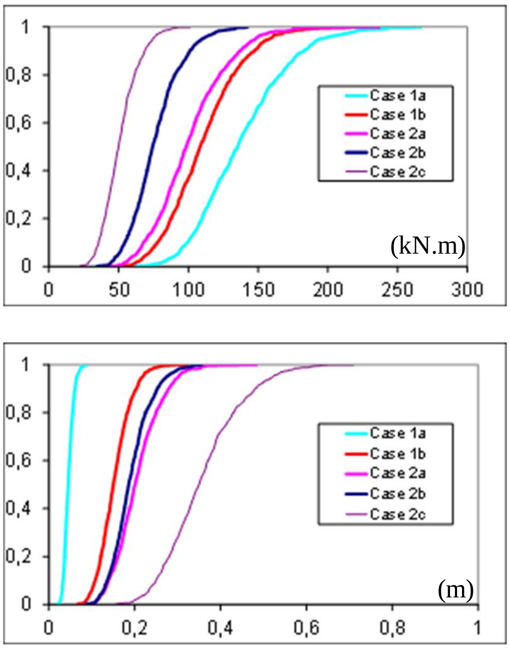

Figure 7: CDF functions for the five cases of: a) bending moments, b) displacements

One can see from the table that the displacement are the highest for the case 2c. The reason for this is attributed firstly to the presence of two different soils and also to the gradient in the correlation length (ratio of 10 between the soft and stiff soils). Conversely, and as previously expected, the maximal bending moment is the largest in the case 1a.

6.3. Effects of Coherency function

In order to study the effect of the spatial correlation of ground motion, three cases of spatially correlated excitation are examined in the study:

- Case 3: fully coherent,
- Case 4: partially incoherent,
- And Case 5: non-coherent.

Table 1: Mean and standard deviation for the five cases

Case	*Displ. (m)*	*Bend. Mt (kN.m)*
1a	*0.05 (0.01)*	*138.4 (33.1)*
1b	*0.15 (0.04)*	*110.8 (26.8)*
2a	*0.19 (0.04)*	*101.1 (26.6)*
2b	*0.21 (0.05)*	*76.6 (18.3)*
2c	*0.36 (0.09)*	*51.1 (12.8)*

The contribution of the quasi-static component of the response to the overall response is significant for displacement response, whereas for bending moment the contribution of the quasi-static response is less prevalent. The maximal responses of the pipe for the three cases are shown in Table 2. It is seen from the table that for the case of uncorrelated ground motion, the responses are higher than those for the case of fully correlated ground motion (almost twice). The reason for this is attributed to the contribution of the quasi-static part of the response. For partially correlated ground motion, the responses are in between the two cases.

Table 2: Effect of the spatial correlation of ground motion on the maximal responses

Case	*Displ. (m)*	*Bend. Mt (kN.m)*
3	*0.13 (0.02)*	*67.8 (15.1)*
4	*0.17 (0.02)*	*97.6 (27.3)*
5	*0.28 (0.03)*	*134.0 (44.0)*

6.4. Effect of the joint-pipe stiffness ratio

The effect of joints on the behavior of the system was analyzed by varying the joint-pipe dimensionless ratio r_{joint} :

$$r_{joint} = \frac{R_j L_P}{E_p I_P} \qquad (17)$$

From a value of 10^{-5} (corresponding to a very soft joint) to 10^{+5} (case of a total transmission of loads) on the basis of the case 1a. It is interesting to underline the strong influence of the joints stiffness since the rigid joints are penalizing by the fact that they necessarily induce more significant stresses. On the other hand, the flexible joints are penalizing with the service limit state if considered. One has to choose an intermediate joint stiffness in order to carry out the best compromise (Table 3). Finally, one can also note that for a given value of r_{joint}, as well as displacements than bending moments decrease with the increase of soil variability.

Table 3: Effect of the joint-pipe stiffness on the maximal responses

r_{joint}	*Displ. (m)*	*Bend. Mt (kN.m)*
10^{-5}	0.41 (0.08)	62.5 (13.8)
10^{-2}	0.22 (0.03)	93.5 (21.2)
10^{2}	0.05 (0.01)	138.4 (33.1)
10^{5}	0.03	197.4 (43.2)

7. CONCLUSION

Following a parametric study, several conclusions are drawn:

Soil heterogeneity induces main effects (differential settlements, bending moments, stresses and possible cracking) that cannot be predicted if soil homogeneity is assumed. The spatial variation of the ground motion could increase or decrease locally the structural response and the magnitude of the induced stresses. This depends also on the soil variability (the soil fluctuation scale), the soil-structure interaction and the pipe-joint stiffness ratio in segmented pipes. Worst case, corresponding to the case leading (from a statistical point of view) to the (statistically) largest effects in the structure, can be found. This kind of approach can give experts new tools for better calibration of safety in soil-structure interaction problems, when the variability of the soil properties associated with the spatial variability of the seismic ground motion are likely to have influence on the responses.

8. REFERENCES

Datta T. K. (2010), Seismic analysis of structures, John Wiley & Sons.

Der Kiureghian, A. (1996) ñA coherency model for spatially varying ground motionsò, Earthquake engineering and structural dynamics, 25(1), 99-111.

Der Kiureghian A., Neuenhofer A. (1992) ñResponse spectrum method for multi-support seismic excitationsò, Earth. Eng. and Struc. Dyn., 21, 713ï 740.

Elachachi S.M., Breysse D., Benzeguir H. (2010) ñSoil spatial variability and structural reliability of buried networks subjected to earthquakesò, Comp. Meth. Stoch. Dyna., ECCOMAS, Ed. M. Papadrakakis, G. Stefanou, V. Papadopoulos, 111-128, Springer.

Eurocode 8, (2005), ñDesign of structures for earthquake resistance ï Part 1: General rules, seismic actions and rules for buildingsò, CEN.

Harichandran R.S., Vanmarke E. (1986) ñStochastic variation of earthquake ground motion in space and timeò, Jour. Eng. Mechanics (ASCE), 112, 154ï 174.

Harichandran R.S., Weijun Wang (1990) ñResponse of indeterminate two span beam to spatially varying seismic excitationò, Earth. Engng Struct Dyn, 19,173ï 187.

Hindy and M. Novak (1980) ñPipeline response to random ground motion,ò Jour. Eng. Mech. Division, ASCE, 106, 339ï 360.

McKay M.D., Beckman R.J, Conover W.J. (1979). ñA Comparison of Three Methods for Selecting Values of Input Variables in the Analysis of Output from a Computer Codeò, Technometrics, 21 (2), 239ï 245.

Navarra G., Barone G., Iacono F. (2013) ñStochastic seismic analysis by using an analytical model of PSD consistent with Response Spectraò, Cong. on Recent Adv. Earth. Eng. and Struct. Dynamics, 28-30 August 2013, Vienna, Austria.

Soliman H.O., Datta TK (1994) ñResponse of continuous beam bridges to multiple support ground motion. Jour. Europ Assoc Earthq Engng, 2, 31ï 44.

VanMarcke, E.(1983) ñRandom Fields: Analysis and Synthesisò, M.I.T. Press, Cambridge, MA.

Zerva A. (2009), ñSpatial variation of seismic ground motions: modeling and engineering applicationsò, CRC Press Group Taylor & Francis.